eLIFE
elifesciences.org

Figures and figure supplements

Matrix metalloproteinase 14 is required for fibrous tissue expansion

Susan H Taylor, et al.

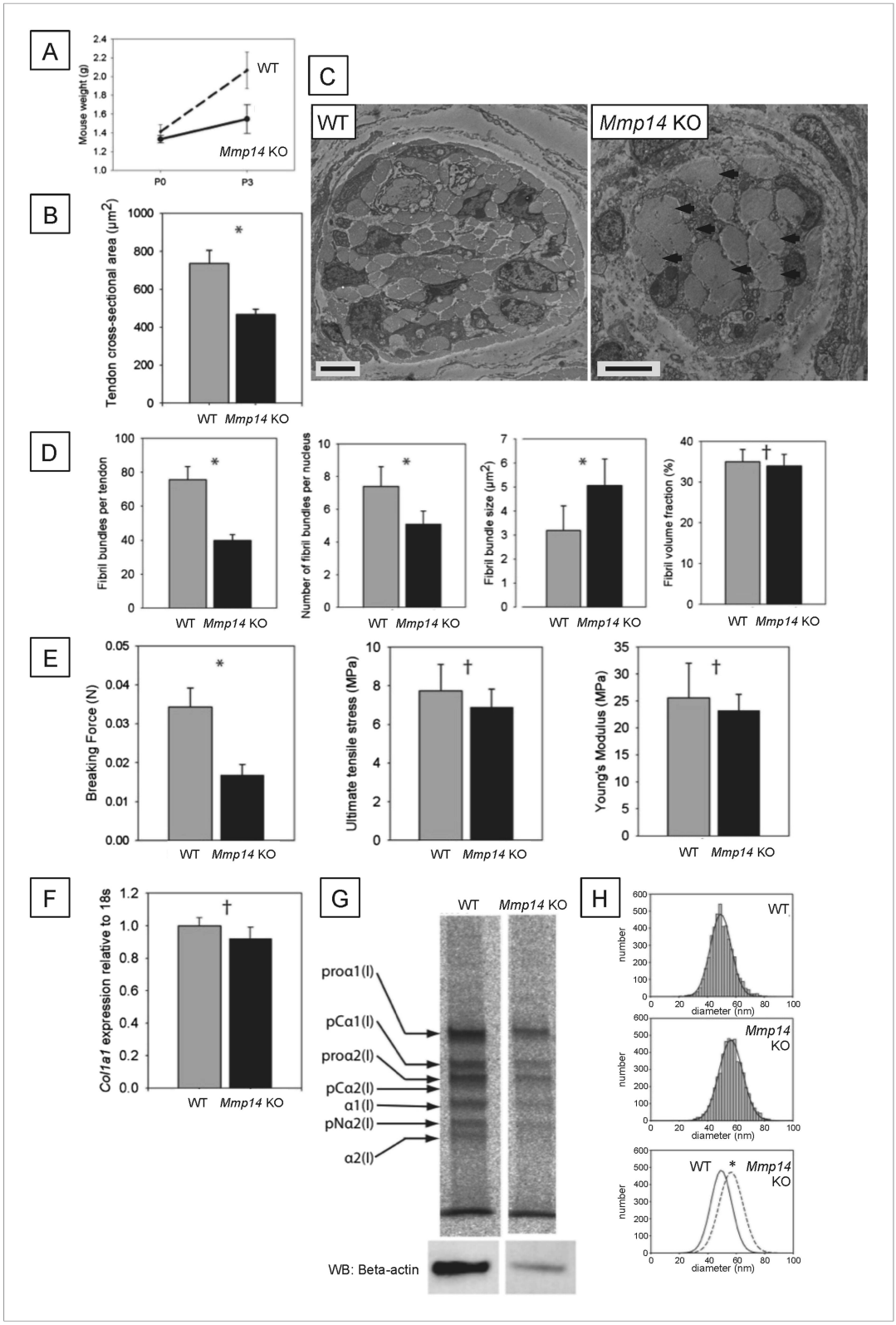

Figure 1. Neonatal *Mmp14*-deficient mice have small and weak tendons. (**A**) Weight of wild type (WT) and *Mmp14* knockout (*Mmp14* KO) littermates at birth (P0) and at 3 days postnatal (P3). (**B**) The cross-sectional transverse area of P0 *Mmp14* KO tendons is significantly smaller than WT tendons. (**C**) TEM images of P0 tail tendon demonstrate that KO tendons are smaller and show dysmorphic, enlarged bundles of collagen fibrils (arrowhead). Scale bars 5 μm.

Figure 1. continued on next page

Figure 1. Continued

(**D**) KO tendons have fewer, larger fibril bundles, but the FVF is not different to WT tendons. (**E**) KO tendons are weaker than WT tendons but have normal mechanical properties after adjusting for differences in size. (**F**) Analysis of *Col1a1* mRNA by qPCR in P0 tendons revealed no difference in gene expression. (**G**) ^{14}C-proline labeling of collagen demonstrated normal collagen processing at P7 in WT and KO tail tendon. (**H**) Fibril diameter distributions of KO and WT tail tendon at P0 revealed significantly increased fibril diameters in KO mice. Bars show SEM. *$p < 0.05$, $^{\dagger}p > 0.05$ (t-tests).

DOI: 10.7554/eLife.09345.003

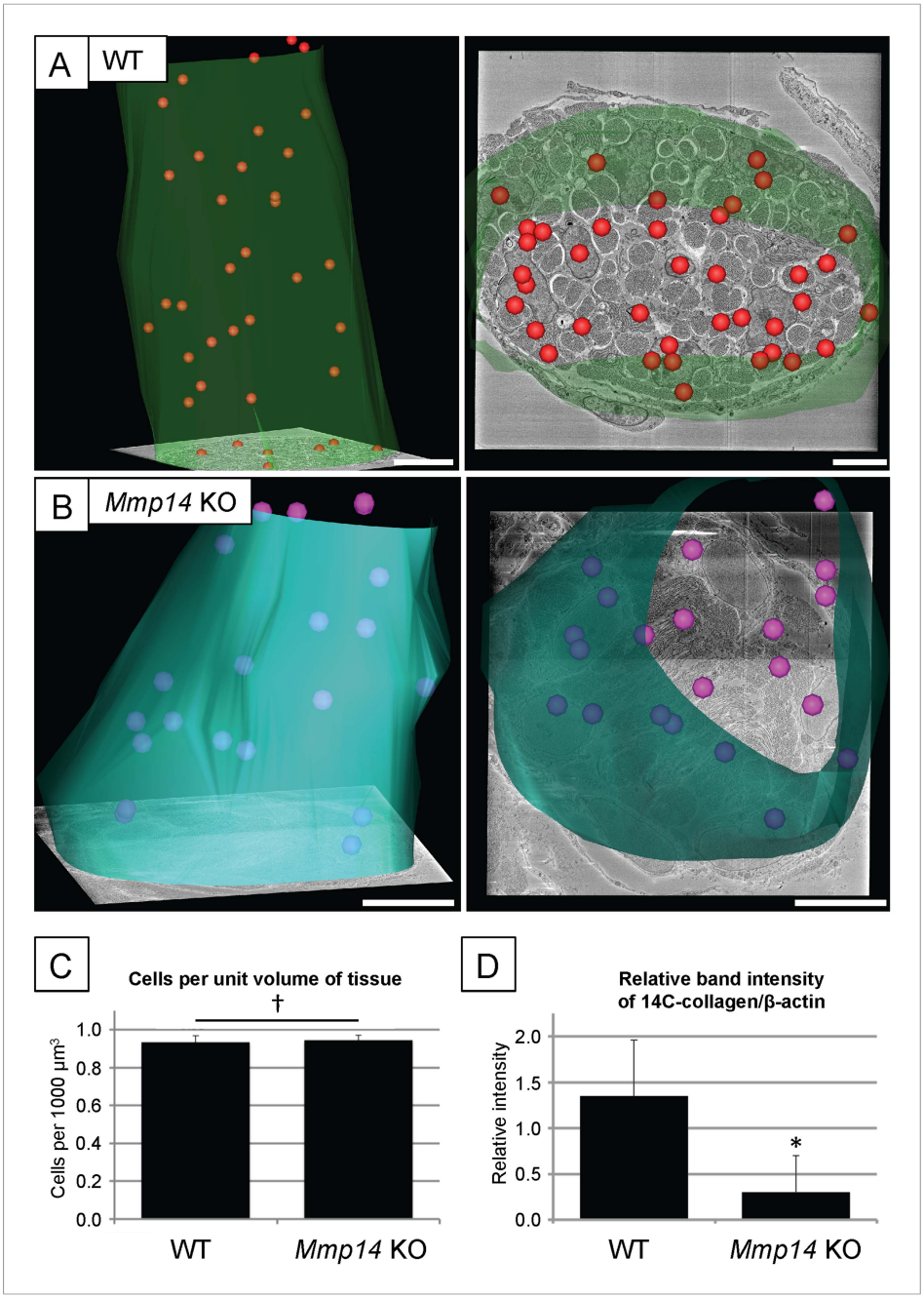

Figure 1—figure supplement 1. Cell number and type I collagen synthesis in neonatal WT and *Mmp14* KO tail tendon. 3D reconstruction from SBF-SEM analysis of P0 (**A**) WT and (**B**) *Mmp14* KO tendons. Green/turquoise, outline of the tendon. Red/pink spheres, cell nuclei. Scale bars 10 µm. (**C**) Estimated mean cell number per unit volume of tissue shows that the absence of MMP14 does not affect cell number at birth. Bars show SEM. $^{\dagger}p > 0.05$ (t-test). (**D**) Densitometry data for P7 tail tendons were labeled with ^{14}C-proline for 1 hr and separate extracellular and intracellular extracts prepared as described (***Canty et al., 2004***). A significant decrease in [^{14}C]-collagen relative to β-actin (detected by western blotting) in the intracellular extracts was observed in the KO samples ($^{*}p < 0.01$, t-test).
DOI: 10.7554/eLife.09345.004

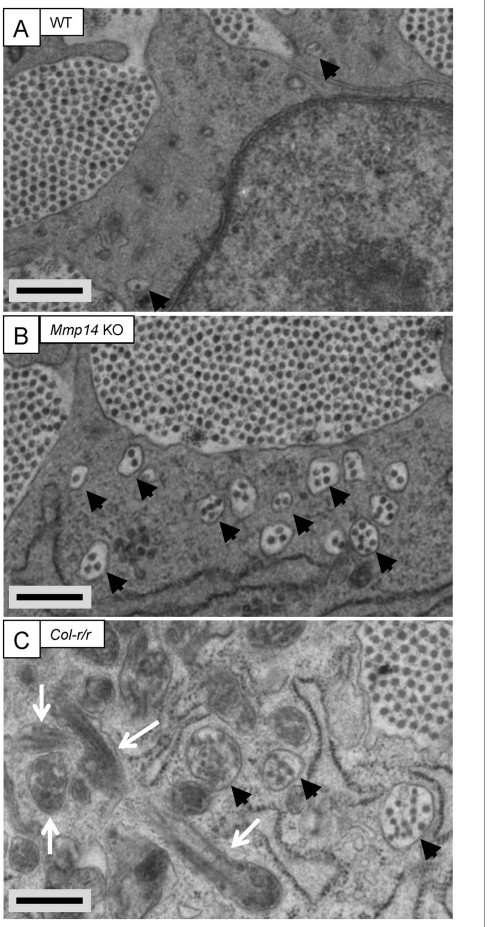

Figure 2. Fibricarrier analysis of wild-type, *Mmp14* KO, and *Col-r/r* embryonic tail tendon. Tail tendons at E15.5 of development from (**A**) wild-type, (**B**) *Mmp14* KO, and (**C**) *Col-r/r* mice. Black arrowhead, recessed fibripositor (electron lucent)-containing collagen fibrils. White arrow, enclosed electron-dense compartment. Scale bars 500 nm.

DOI: 10.7554/eLife.09345.005

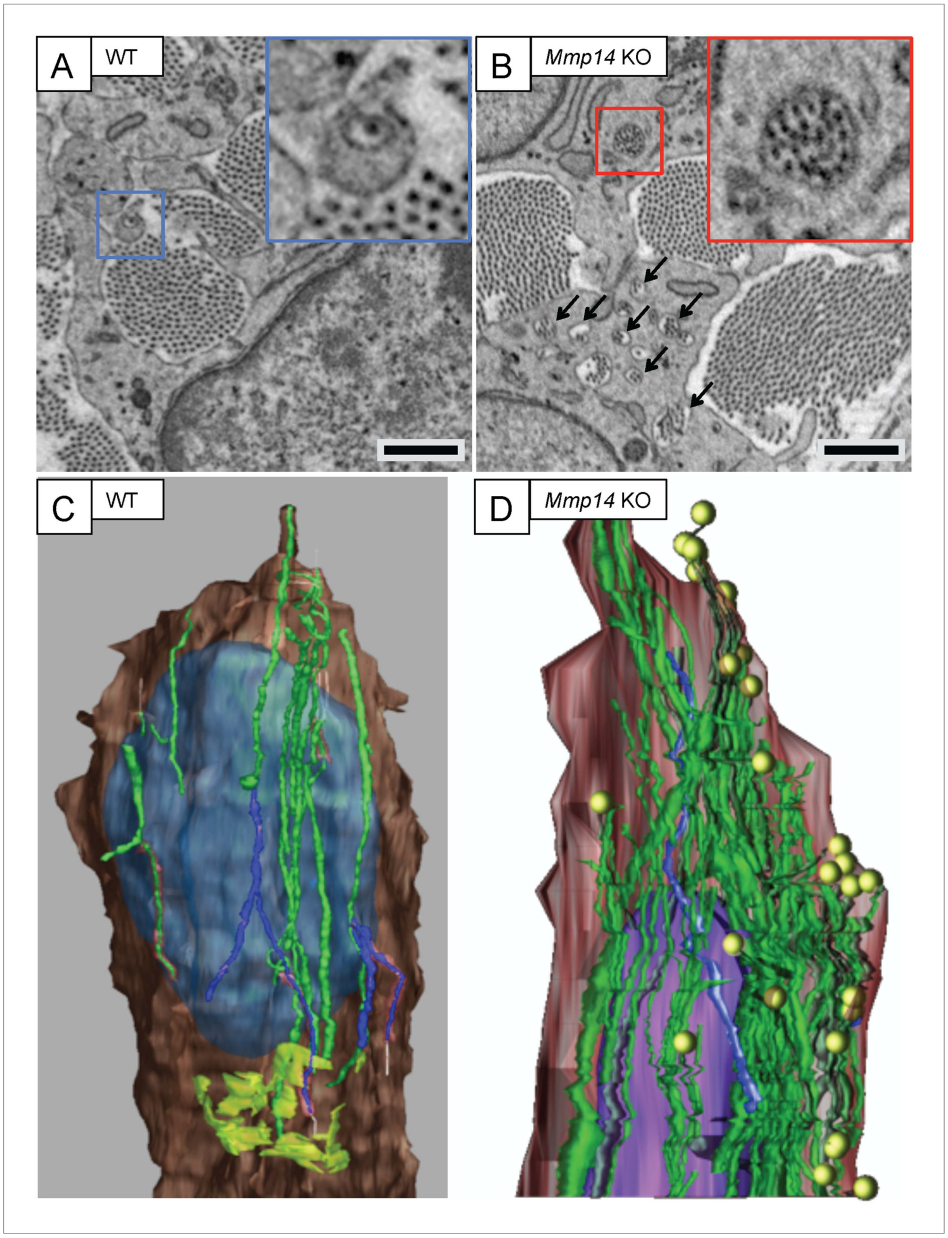

Figure 2—figure supplement 1. *Mmp14*-deficient mice have prominent recessed fibripositors. SBF-SEM of (**A**) WT and (**B**) *Mmp14* KO tendons at E15.5 showing fibripositors in WT tendons (blue box) and intracellular collagen fibril-containing compartments in *Mmp14* KO tendons (red box; arrowheads). Scale bars 1 μm. 3D reconstruction of SBF-SEM data from (**C**) WT and (**D**) *Mmp14* KO tendon cells. Brown, cytoplasm. Purple/blue, nucleus. Green, internal collagen fibril compartments. Yellow circles, fibril ends. Lime green (in WT only), Golgi apparatus.
DOI: 10.7554/eLife.09345.006

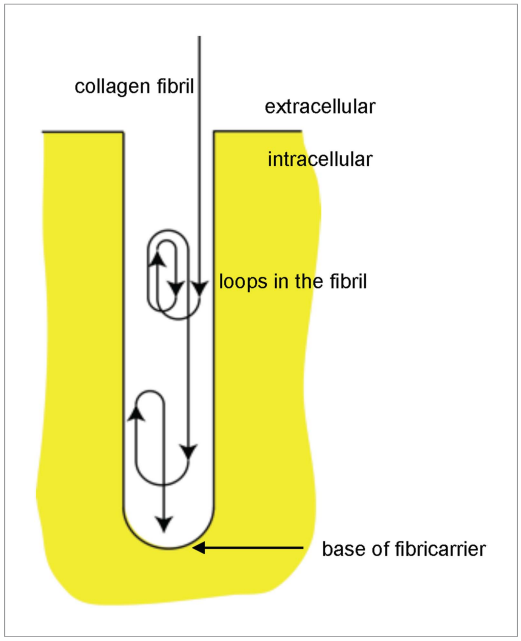

Figure 2—figure supplement 2. Schematic showing looping of collagen fibrils in recessed fibripositors. Diagrammatic representation of a recessed fibripositor with looping of a collagen fibril. Not drawn to scale.
DOI: 10.7554/eLife.09345.007

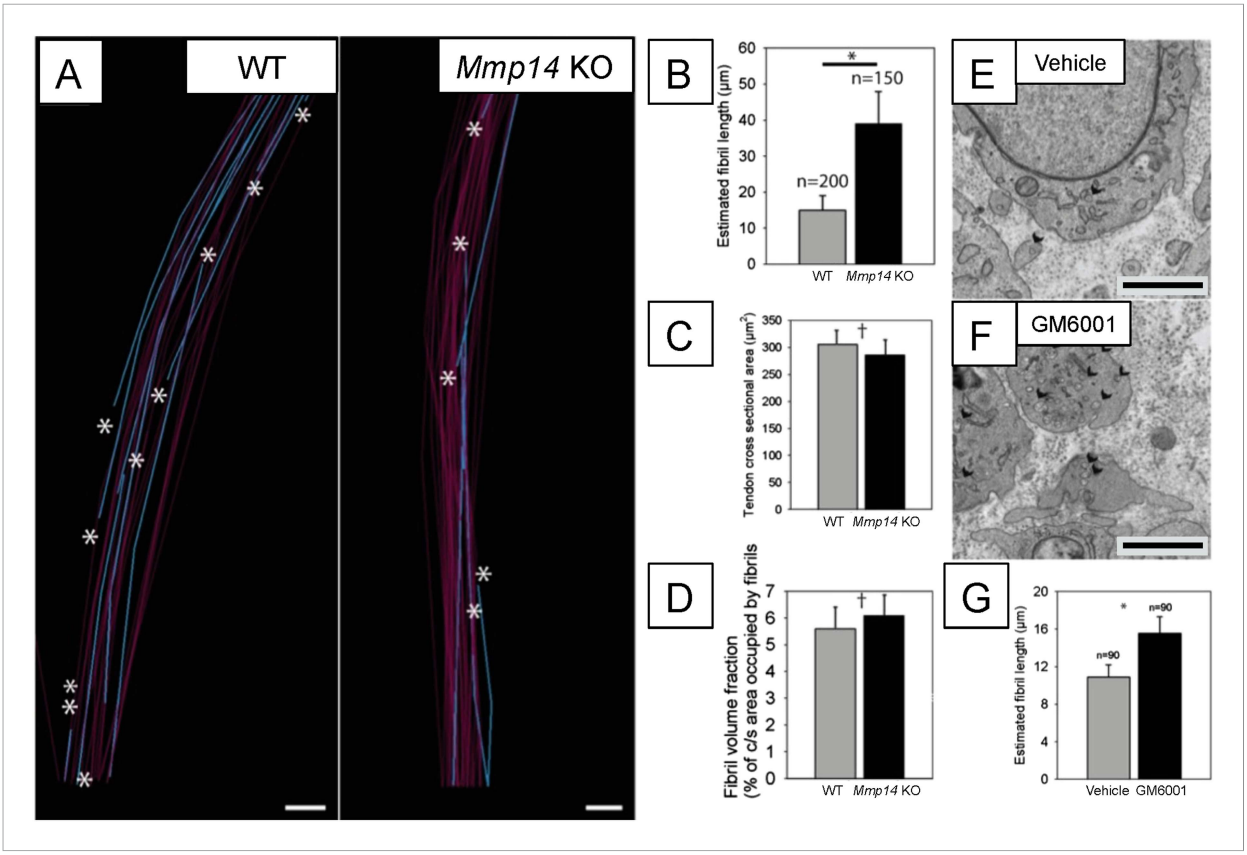

Figure 3. Deficiency in MMP14 activity results in fewer collagen fibrils. (**A**) 10 μm-deep (z-axis) slices of 3D reconstructions of SBF-SEM data taken from of WT and *Mmp14* KO embryonic tendons at E15.5 showing collagen fibrils (blue) with a tip (marked by asterisks) found within the volume. Purple fibrils passed through the volume and so did not have tips in the reconstruction. Scale bars 500 nm. (**B**) Quantification of mean fibril length based on the number of tips identified shows that E15.5 WT fibrils are shorter than fibrils in age- and anatomical position-matched tail tendons from KO mice (308 and 266 fibrils tracked, respectively). (**C**) Tendon cross-sectional area and (**D**) FVF are not different at E15.5 KO tendons. (**E**, **F**) Electron microscopy of tendon-like constructs cultured in the presence of MMP inhibitor GM6001 (10 μM in 0.1% DMSO) show increased number of recessed fibripositors (arrowheads) compared to vehicle control. Scale bars 1 μm. (**G**) Increase in calculated mean fibril length in GM6001-treated tendon-like constructs. Bars show SEM. *$p < 0.05$, †$p > 0.05$ (t-tests).

DOI: 10.7554/eLife.09345.010

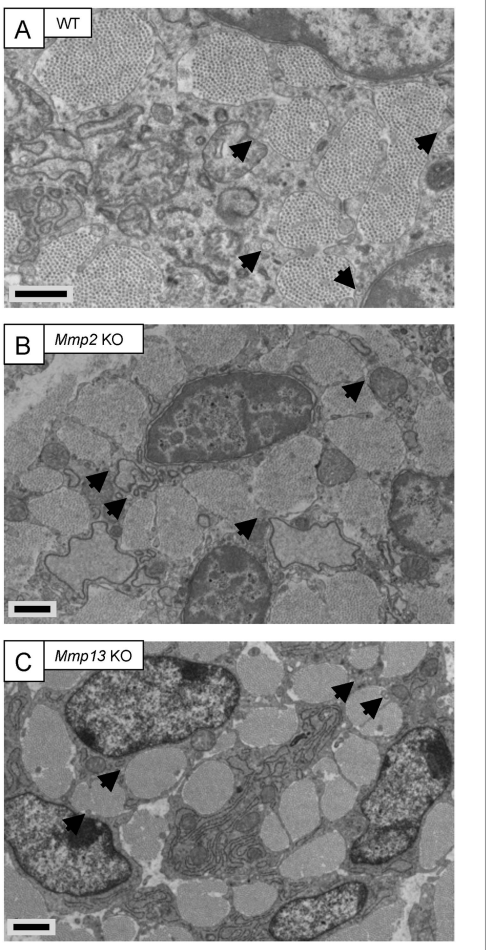

Figure 3—figure supplement 1. Embryonic tendons deficient in *Mmp2* or *Mmp13* do not have overt tendon phenotypes. Electron microscopy images of embryonic tendons from (**A**) WT, (**B**) *Mmp2* KO, and (**C**) *Mmp13* KO mice. Arrowheads indicate the locations of fibripositors. Scale bars 1 μm.

DOI: 10.7554/eLife.09345.011

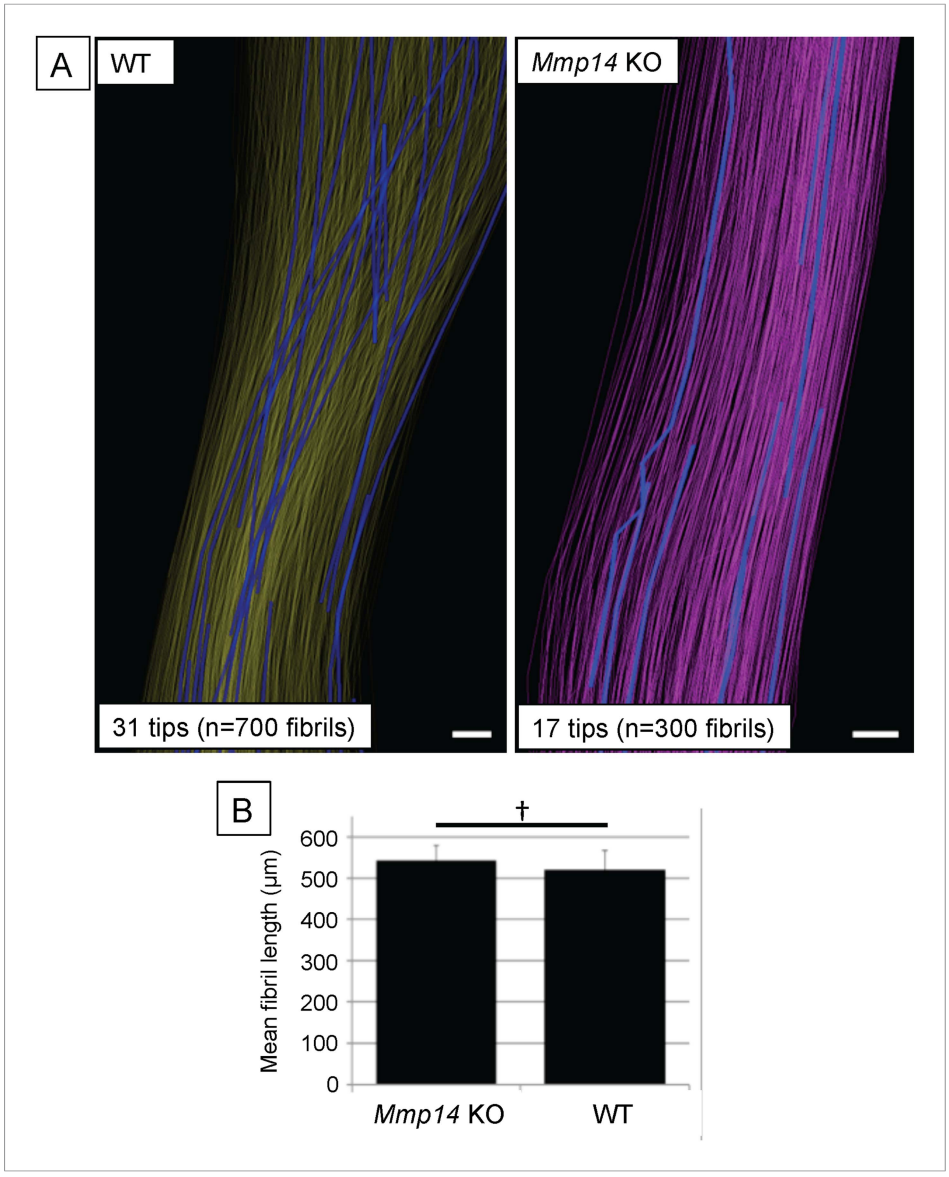

Figure 3—figure supplement 2. Deficiency in MMP14 activity results in fewer collagen fibrils tips at P0. (**A**) 3D reconstruction from SBF-SEM analysis of P0 WT and *Mmp14* KO tendons. Scale bars 2 µm. (**B**) Estimated mean fibril length 645 ± 14 µm WT and 674 ± 24 µm *Mmp14* KO shows that the absence of MMP14 does not affect fibril length at birth. Bars show SEM. $^{\dagger}p > 0.05$ (t-test).

DOI: 10.7554/eLife.09345.012

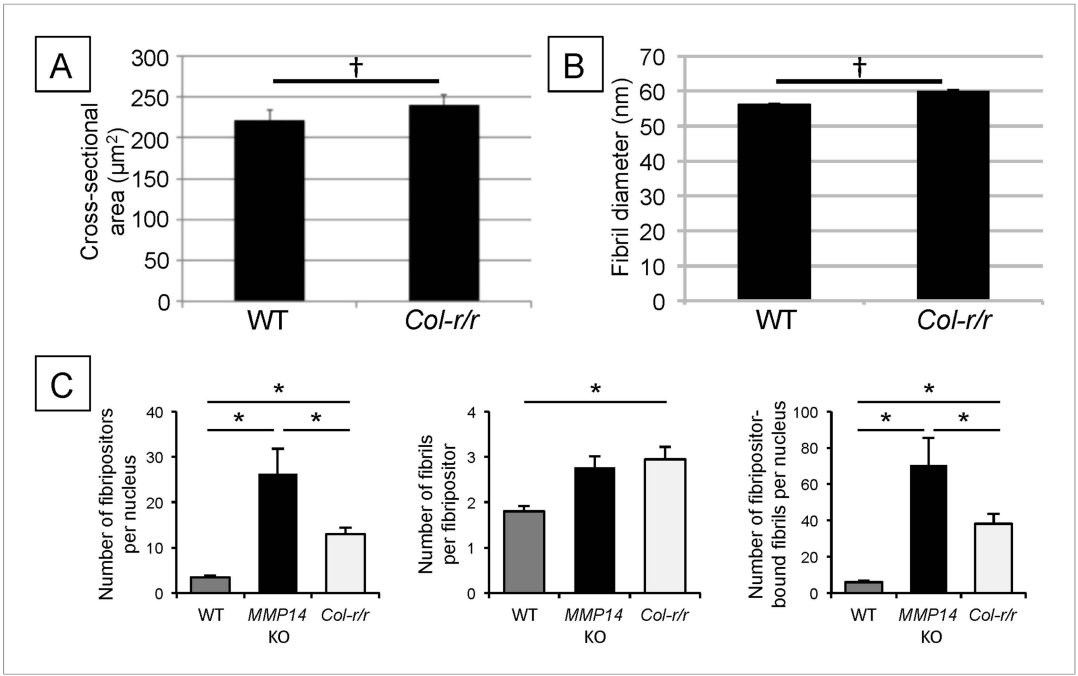

Figure 3—figure supplement 3. Quantitative analysis of *Col-r/r* embryonic tendons. Measurement of tendon cross-sectional area (**A**) and collagen fibril diameter (**B**) shows no significant difference between WT and *Col-r/r* mice at E15.5. †$p > 0.05$ (t-tests). (**C**) Quantitation of fibril-containing carriers in WT, *Mmp14* KO, and *Col-r/r* embryonic tenocytes. *$p < 0.05$ (one-way ANOVA). Bars show SEM.

DOI: 10.7554/eLife.09345.013

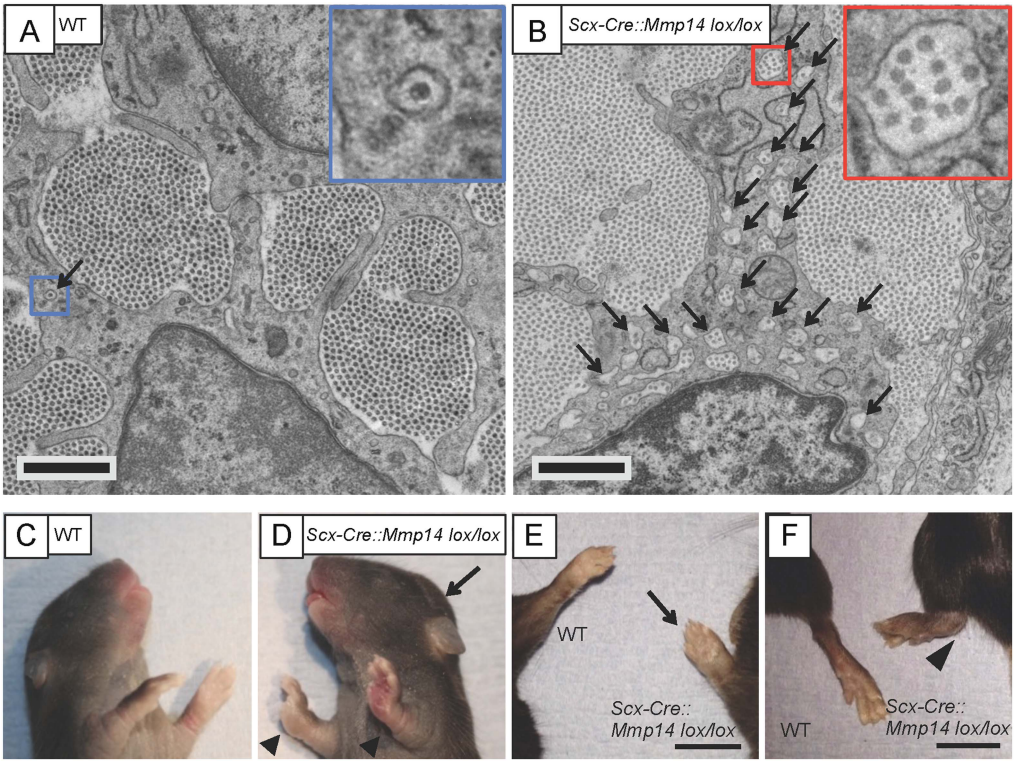

Figure 4. *Scx-Cre::Mmp14 lox/lox* mice have limb and skeletal deformities. Tail tendons from littermates at P0 from (**A**) WT and (**B**) *Scx-Cre::Mmp14 lox/lox* mice show *Mmp14*-null tendons have multiple fibripositors-containing multiple fibrils (red box) than fibripositors in WT tendons (blue box). Black arrowhead, recessed fibripositor (electron lucent)-containing collagen fibrils. Scale bars 500 nm. (**C**) Control pups at P8 showed normal limb development but (**D**) *Scx-Cre::Mmp14 lox/lox* littermates show dorsiflexion of their limbs (arrowhead) and dome-shaped skull (arrow). Adult (7 week old) *Scx-Cre::Mmp14 lox/lox* mice have (**E**) enlarged paws (open arrow) and (**F**) extreme dorsiflexion of hind limbs (arrowhead) compared to control littermates. Scale bars 1 cm.

DOI: 10.7554/eLife.09345.015

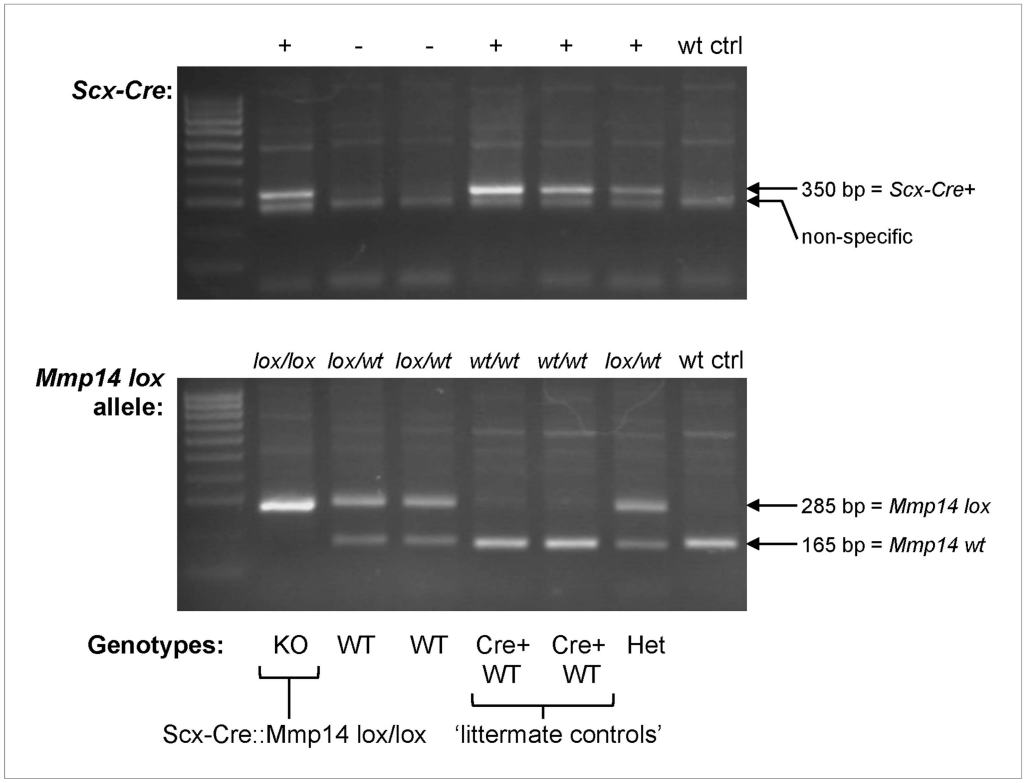

Figure 4—figure supplement 1. Genotyping the *Scx-Cre::Mmp14 lox/lox* colony. A typical genotyping result to identify *Scx-Cre::Mmp14 lox/lox* mice. Wt ctrl, control wild-type DNA. Het, heterozygous (*lox/wt, Cre+*). KO, homozygous knockout (*lox/lox, Cre+*). WT, wild-type (no Cre). Cre+ WT, Cre-expressing WT (*wt/wt, Cre+*) used as controls.

DOI: 10.7554/eLife.09345.016

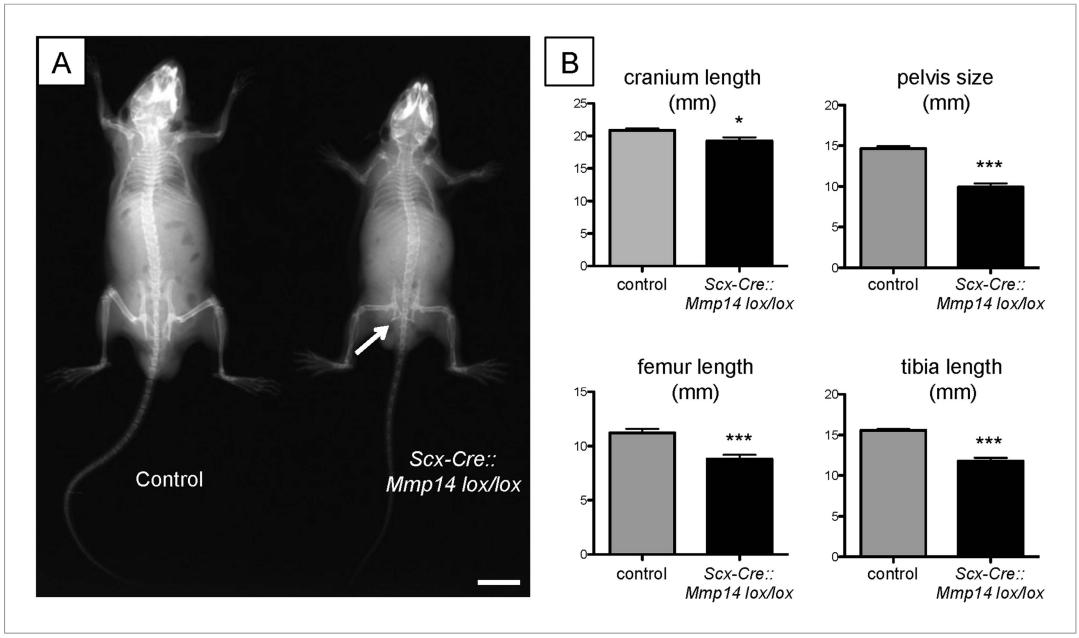

Figure 4—figure supplement 2. Adult *Scx-Cre::Mmp14 lox/lox* mice have skeletal deformities. (**A**) Representative x-ray shows adult (7 weeks old) *Scx-Cre::Mmp14 lox/lox* mice are smaller than control littermates and have reduced bone density. White arrow indicates hip dysplasia. Scale bars 1 cm. (**B**) 7-week-old *Scx-Cre::Mmp14 lox/lox* mice have shorter cranium length, smaller pelvis, and shorter long bones. Bars show SEM. *p = 0.0105; ***p < 0.001 (t-tests; 12 control, 8 *Scx-Cre::Mmp14 lox/lox*).

DOI: 10.7554/eLife.09345.017

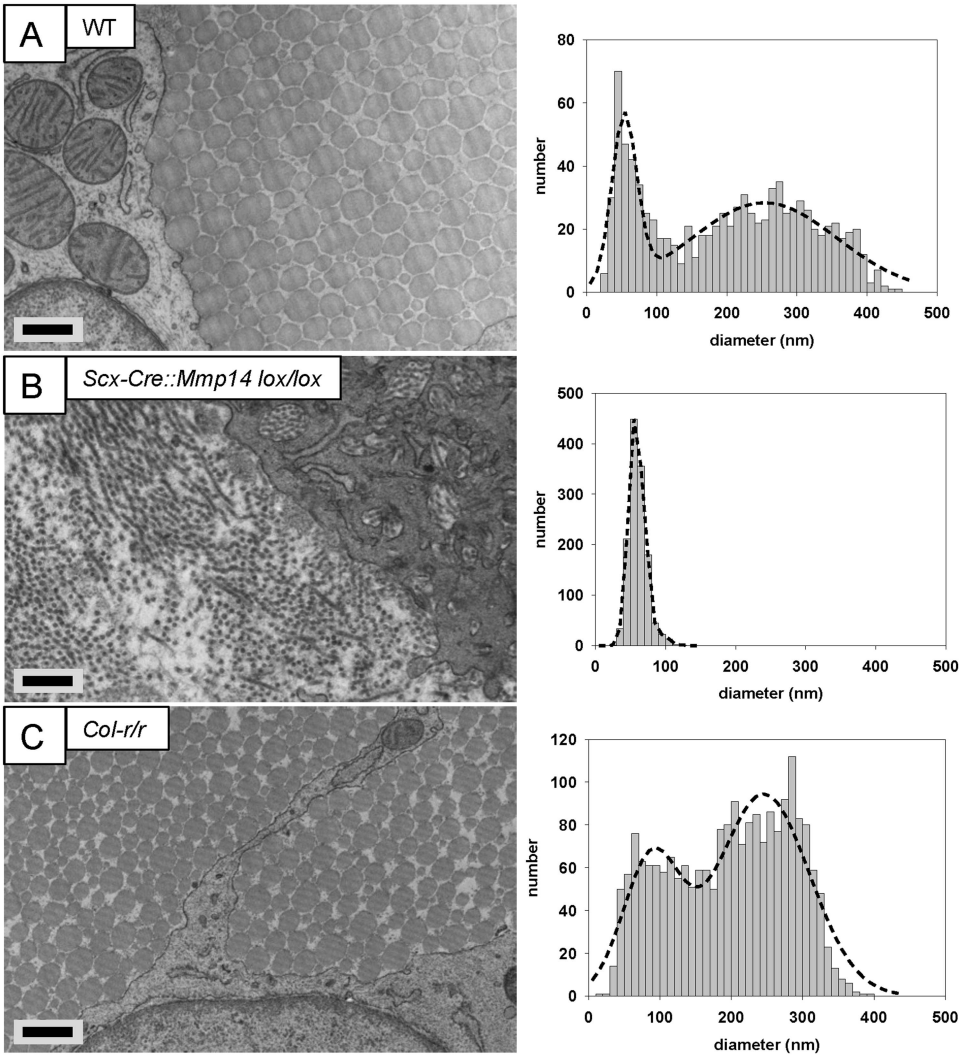

Figure 5. Deficiency in MMP14 activity inhibits bimodal fibril diameter distribution in tendons from adult mice. Tail tendons from 7 week-old (**A**) WT, (**B**) *Scx-Cre::Mmp14 lox/lox*, and (**C**) *Col-r/r* mice. Larger diameter fibrils can be observed in the ECM of WT and *Col-r/r* postnatal tendons but only narrow diameter fibrils are observed in *Mmp14*-deficient postnatal tendons. Scale bars 500 nm.

DOI: 10.7554/eLife.09345.018

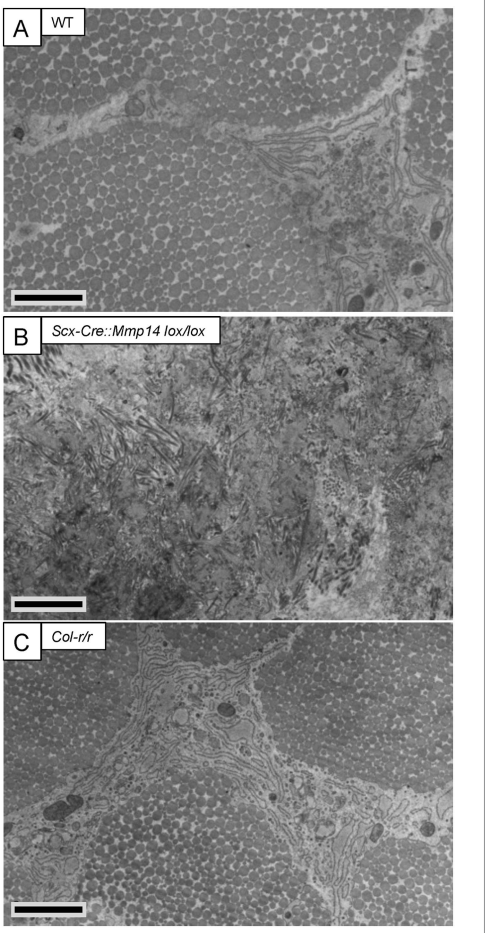

Figure 5—figure supplement 1. Cleavage of the -¼ collagen-I site is not required for release of fibrils in tendons from adult mice. Electron microscopy images of tendons from 7-week-old (**A**) WT, (**B**) *Scx-Cre::Mmp14 lox/lox*, and (**C**) *Col-r/r* mice. Larger diameter fibrils occur in the ECM of WT and *Col-r/r* postnatal tendons but only narrow diameter fibrils occur in *Mmp14*-deficient postnatal tendons. Scale bars 2 μm.
DOI: 10.7554/eLife.09345.019

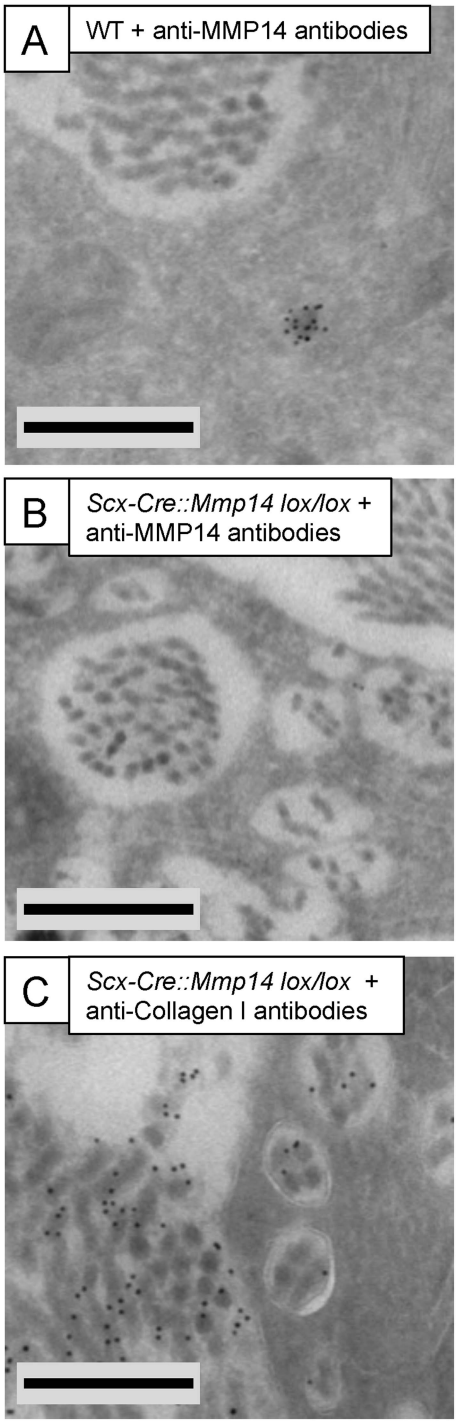

Figure 5—figure supplement 2. Immuno-electron microscopy of *Scx-Cre::Mmp14 lox/lox* tendon. (**A**) WT and (**B**) *Scx-Cre::Mmp14 lox/lox* tail tendon from P7 (7 days) mice were labeled with anti-MMP14 antibody. (**C**) *Scx-Cre::Mmp14 lox/lox* tendon labeled with anti-collagen-I antibody. Scale bars 500 nm.
DOI: 10.7554/eLife.09345.020

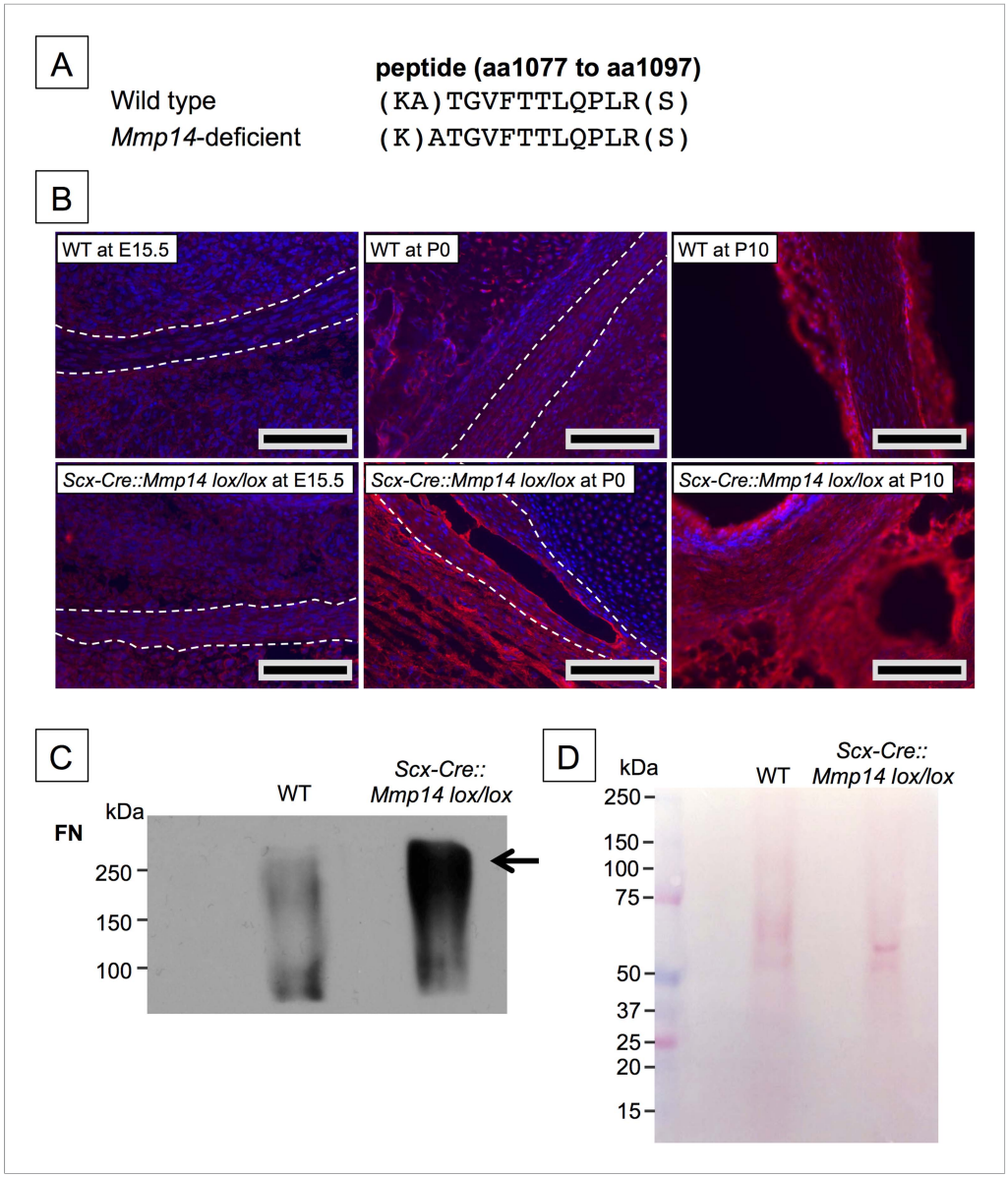

Figure 6. Elevated FN in *Mmp14*-deficient tendons. (**A**) Sequence of a unique semi-tryptic peptide of FN identified in neonatal (P7-10) WT tendon and the sequence of the corresponding peptide from *Mmp14*-deficient tendons without the additional Ala(1078)-Thr(1079) cleavage. (**B**) Immunofluorescence analysis of FN in tendons of WT and *Scx-Cre::Mmp14 lox/lox* mice at E15.5, P0, and P10 of development. Scale bars 200 μm. (**C**) Western blot analysis of P7 WT and *Scx-Cre::Mmp14 lox/lox* tendons show elevated FN in *Mmp14*-deficient tendons. (**D**) Ponceau S-stained membrane shows equivalent extractability of WT and *Scx-Cre::Mmp14 lox/lox* tendons.

DOI: 10.7554/eLife.09345.021

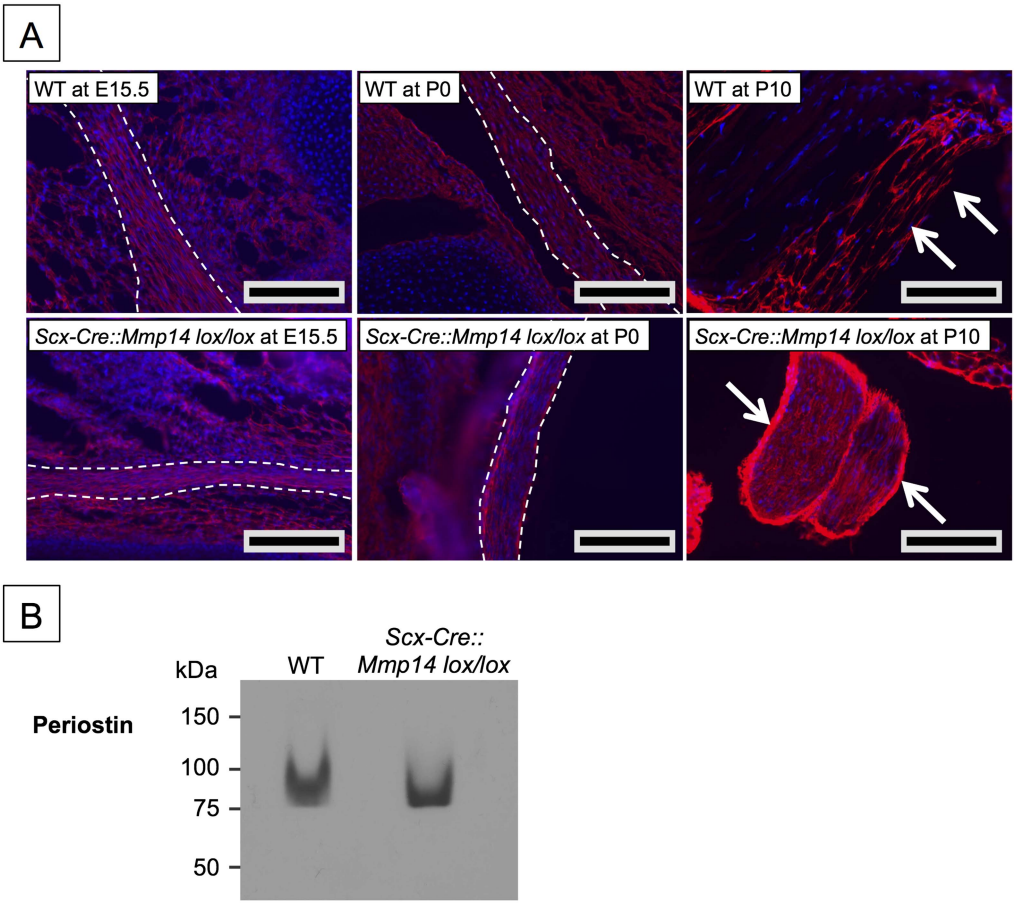

Figure 6—figure supplement 1. Elevated periostin levels only in postnatal *Scx-Cre::Mmp14 lox/lox* tendons. (**A**) Immunofluorescence analysis of periostin in tendons of WT and *Scx-Cre::Mmp14 lox/lox* mice at E15.5, P0, and P10 of development show accumulation of periostin in epithelium (white arrows) of *Scx-Cre::Mmp14 lox/lox* tendons. Scale bars 200 μm. (**B**) Western blot analysis of P7 WT and *Scx-Cre::Mmp14 lox/lox* Achilles tendons show similar levels of periostin in *Mmp14*-deficient tendons.

DOI: 10.7554/eLife.09345.022

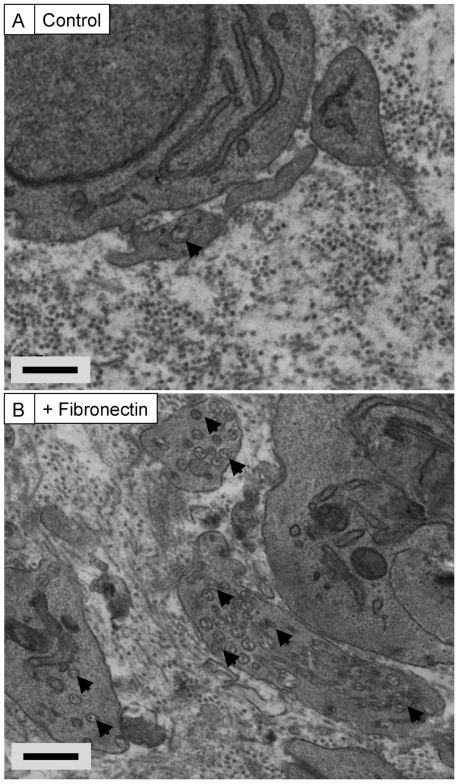

Figure 6—figure supplement 2. Exogenous FN induces recessed fibripositors in tendon-like constructs. Transmission electron microscopy of tendon-like constructs in the absence (**A**) and presence (**B**) of 200-μg/ml human plasma fibronectin. Arrowheads show recessed fibripositors, which were abundant in the treated constructs. Scale bars 500 nm.

DOI: 10.7554/eLife.09345.023